Characterization of New Sulfide Ions ($C_2S_3^{\bullet+}$) from Ethenedithione by Ion−Molecule Reactions

Pascal Gerbaux and Robert Flammang*

Organic Chemistry Laboratory, University of Mons-Hainaut, B-7000 Mons, Belgium

Carl Th. Pedersen

Department of Chemistry, Odense University, DK-5230 Odense, Denmark

Ming Wah Wong*

Department of Chemistry, The National University of Singapore, Kent Ridge, Singapore, 119260

Received: October 22, 1998; In Final Form: February 8, 1999

Collisional activation (high or low translational energy) and neutralization−reionization mass spectrometries appear inefficient for the characterization of the connectivity of isomeric $C_2S_3^{\bullet+}$ ions generated by dissociative ionization of 1,2-dithiolo[4,3-*c*][1,2]dithiole-3,6-dione (**1**), 1,2-dithiolo[4,3-*c*][1,2]dithiole-3-one-6-thione (**2**), and 1,3,4,6-tetrapentalene-2,5-dione (**3**). In contrast, ion−molecule reactions (particularly with nitric oxide) readily differentiate the *C*-sulfide ethenedithione ion, $SCCS_2^{\bullet+}$ (**4**), and the *S*-sulfide ethenedithione ion, $SCCSS^{\bullet+}$ (**5**). The collisional activation spectra of these ion−molecule reaction products have been recorded on a new type of hybrid tandem mass spectrometer of sectors−quadrupole−sectors configuration. The characterization of the isomeric $C_2S_3^{\bullet+}$ ions is supported by ab initio calculations at the G2(MP2,SVP) level. The *C*-sulfide ethenedithione ion is predicted to be more stable than the *S*-sulfide form by 91 kJ mol^{-1}. The calculated reaction enthalpies for the two isomeric forms $C_2S_3^{\bullet+}$ with nitric oxide support the characterization by ion−molecule reactions.

Introduction

During the study of the behavior of dithiolodithioles upon flash vacuum pyrolysis (FVP) making use of matrix isolation infrared spectroscopy and tandem mass spectrometry,[1] it was noticed that, following dissociative electron ionization of **1** and **2**, unexpected ion species were generated at *m*/*z* 116 for **1** and *m*/*z* 132 for **2**. High-resolution mass measurements have confirmed the composition of these species as C_3OS_2 and C_3S_3, respectively and applications of tandem mass spectrometric methodologies have supported the OCCCSS and SCCCSS connectivities (Scheme 1).

Carbon monoxide is indeed readily expelled from the molecular ions of the dithiolodithioles **1** and **2** and, in a consecutive reaction, the intermediate radical cations eliminate disulfur. Another competitive reaction consists of the loss of carbon disulfide or carbon oxysulfide producing $C_2S_3^{\bullet+}$ radical cations (*m*/*z* 120). If the mechanisms depicted in Scheme 1 are correct, one may expect the formation of ethenedithione *S*-sulfide ions, $S{=}C{=}C{=}S^+{-}S^\bullet$ (**5**). In fact, the isomeric dithiolodithiole **3** is also an excellent precursor of $C_2S_3^{\bullet+}$ radical cations,[2] and given the arrangement of the atoms in the neutral precursor, one would expect that its dissociative ionization could produce the isomeric *C*-sulfurated species, $S{=}C{=}CS_2^{\bullet+}$ (**4**).

In connection with our current interest with the chemistry of $C_nS_3^{\bullet+}$ radical cations,[3] we have therefore applied tandem mass spectrometry methodologies to the $C_2S_3^{\bullet+}$ radical cations (*m*/*z* 120) making use of a new type of hybrid mass spectrometer.[4,5] The performed MS experiments include collisional activation (CA) at high (8 keV) and low (ca. 20−30 eV) translational energies of the incident ion beams, neutralization−reionization (NR) experiments, and ion−molecule reactions at near-thermal (∼5 eV) energies. In addition, high-level ab initio calculations were used to elucidate the structures and energies of the isomeric $C_2S_3^{\bullet+}$ ions and to investigate their ion−molecule reactions with nitric oxide.

SCHEME 1

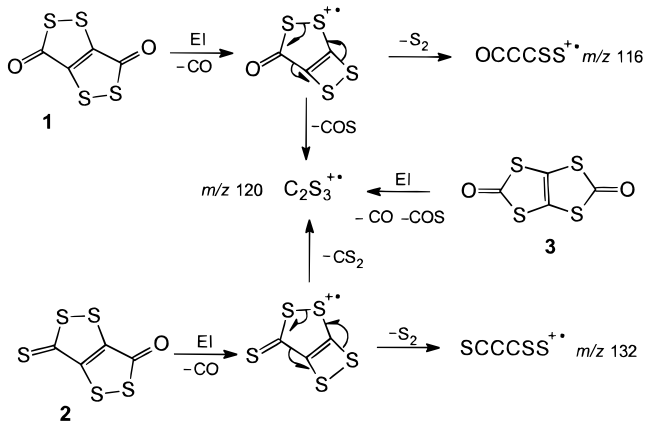

Mass Spectrometric Results

1. Experiment. All the spectra were recorded on a large-scale tandem mass spectrometer (Micromass AutoSpec 6F) combining six sectors of $E_1B_1©E_2©©E_3B_2©E_4$ geometry (E stands for electric sector, B for magnetic sector, and © for the collision cells installed in various field-free regions).[6] In the hybrid mode, the neutralization cell is replaced by a demagni-

10.1021/jp984121l CCC: $18.00
Published on Web 04/24/1999

TABLE 1: CA (8 keV Translational Energy, Oxygen Collision Gas) and NR (Xenon/Oxygen) Spectra of the $C_2S_3^{\bullet+}$ Ions Generated by Dissociative Ionization of the Dithiolodithioles 1−3

	m/z						
precursor	88	76	64	CS[a]	56	44	32
1	23	100	3	1	3	11	1
2	25	100	3	3	4	10	1
3	14	100	2	1	2	11	1
1[b]	21	50	18		14	100	14
2[b]	7	36	7		7	100	19
3[b]	8	100	12		6	81	6

[a] Charge stripping peak (*m/z* 60). [b] NRMS: recovery signal intensity of 2, 1, and 1% for **1**, **2**, and **3**, respectively.

fication lens, and an rf-only quadrupole collision cell (q) fitted with deceleration and acceleration lenses is installed behind E_2 ($E_1B_1©E_2q©E_3B_2©E_4$ configuration).[4,5]

General conditions were 8 kV accelerating voltage, 200 μA trap current, 70 eV ionizing electron energy, and 200 °C ion source temperature. The solid samples **1**−**3** were introduced with a direct insertion probe.

CA (oxygen collision gas) and NR (xenon/oxygen collision gases) spectra were recorded by scanning the field of E_3 and collecting the ions in the fifth field-free region with an off-axis photomultiplier detector, residual non-neutralized ions being removed by floating an intermediate ion source at 9 kV.

Details of the use of this instrument in the hybrid mode have been reported earlier.[4,5] Briefly, the experiments consist of the selection of a beam of fast ions (8 keV) with $E_1B_1E_2$ (MS1), the retardation of these ions at near-thermal energies, and the reaction with a reagent gas at a pressure estimated to be around 10^{-3} Torr. After reacceleration to 8 keV, all the ions present in the quadrupole are separated and mass measured by scanning the field of the second magnet B_2. The high-energy CA spectra of selected ions generated in the quadrupole can also be recorded by a linked scanning of the fields of the last three sectors $E_3B_2E_4$ (MS2) (resolved mode) or a conventional scanning of E_4 after mass selection with B_2. For the low-energy CA spectra, argon was the collision gas in the quadrupole collision cell and the energy of the impinging ions was regulated in order to maximize the yield of the fragment ions.

3,6-Dihydro[1,2]dithiolo[4,3-*c*][1,2]dithiole-3,6-dione (**1**) was prepared according to literature procedure.[7] 1,3,4,6-Tetrathiapentalene-2,5-dione (**3**) was commercially available (Aldrich) and used without further purification.

2. Collisional Activation (CA) and Neutralization−Reionization (NR) Spectra. The high-energy CA spectra of the $C_2S_3^{\bullet+}$ ions formed by dissociative ionization of **1**−**3** are collected in Table 1. All these spectra are characterized by intense peaks at *m/z* 88, 76, and 44 which can be ascribed to both SCCSS and SCC(S)S connectivities. The remaining peaks at *m/z* 64 and 56 are also present in all cases, and the only difference which could be significant is the relative abundance of the doubly charged ions (charge stripping, *m/z* 60), but instrumental parameters such as collector slit width may strongly affect this value.

Neutralization−reionization mass spectrometry (NRMS) has been recognized as a valuable tool for the characterization of reactive neutral molecules in the gas phase.[8] One important characteristic of NRMS is that, due to a high-energy deposition in the reionized species, rearrangement reactions are generally not favored. As a result, NR spectra may be more structure-specific than the CA spectra of isomeric ions. The NR data of the $C_2S_3^{\bullet+}$ radical cations of **1**−**3** are collected in Table 1. The recovery signals are hardly seen in the three cases pointing out an intrinsic instability of the neutral C_2S_3 species or an important geometry difference between the neutral and ionized states (unfavorable Franck−Condon factors).[9] Relative intensity differences of the fragment ions are more pronounced in the NR than in the CA spectra, but difficult to interpret in terms of the structures of the $C_2S_3^{\bullet+}$ ions.

TABLE 2: CA (ca. 20 eV Translational Energy, Argon Collision Gas) of the *m/z* 120 Ions Generated by Dissociative Ionization of 1−3

	m/z					
precursor	88	76	64	56	44	32
1	17	100	8	<1	<1	<1
2	17	100	5	<1	<1	<1
3	6	100	2	<1	<1	<1

In the low kinetic energy regime using argon as the target, the major collision-induced fragmentation yields *m/z* 64 ions and less intense peaks are also observed at *m/z* 44 and 56 (Table 2). These data are again not useful for structure elucidation.

3. Ion−Molecule Reactions. In its hybrid "sectors−quadrupole−sectors" configuration, the AutoSpec 6F mass spectrometer allows also the study of ion−molecule reactions at near thermal energies.[4,5] Such ion−molecule reactions may complement in several instances the collisional activation data. We have therefore investigated the behavior of the $C_2S_3^{\bullet+}$ ions toward several neutral reagents including dimethyl disulfide (DMDS), nitric oxide, acetonitrile, and methyl isocyanide.

Recent works have indeed indicated that dimethyl disulfide (DMDS)[10,11] can be a useful reagent for the characterization of ions presenting a distonic character. Nevertheless, in the present case, the *m/z* 120 ions generated from **1**−**3** react only by charge exchange with the production of ionized DMDS, and peaks corresponding to $CH_3S^{\bullet}$ radical abstraction are not observed.

In contrast to the $OCCCSS^{\bullet+}$ and $SCCCSS^{\bullet+}$ ions which react specifically with nitric oxide producing SNO^+ (*m/z* 62) ions,[1] the behavior of the *m/z* 120 ions of **1** is completely unexpected and appears quite complex, as prominent peaks are now seen at *m/z* 106, 88, 86, 76, and 74 (among these ions, *m/z* 88 and 76 ions are the products of unimolecular fragmentation of metastable *m/z* 120 ions); formation of SNO^+ ions is a minor process (Figure 1a). Given the composition of the reacting ions and the nature of the reagent gas, the composition of the ion−molecule products must be $CNOS_2$, C_2NOS, and CNOS, respectively. High-energy collisional activation has been applied to these unexpected ions by linked scanning of the fields of MS2 ($E_3B_2E_4$) after selecting the mass of the precursor ions with MS1 (Table 3). These CA data suggest that the *m/z* 74 ions have the S═C═N═O connectivity resulting from the displacement of CS_2 by $NO^{\bullet}$. It was surprising at first sight that the base peak of the CA spectrum of the *m/z* 74 ions corresponds to $CS^{\bullet+}$ ions given the fact that the ionization energy of $NO^{\bullet}$ is lower than the ionization energy of CS (9.2 eV viz. 11.3 eV).[12] Production of triplet ONCS ions can explain this peculiar behavior.[13] The *m/z* 86 ions are $SCCNO^+$ ions, isomers of the OCCNS and OCNCS connectivities established previously[14] by collisional activation and the *m/z* 106 ions are also resulting from the displacement of CS by $NO^{\bullet}$. We have recently observed the generation of complexes between nitric oxide and ionized H_2O, H_2S, methanol, alkane thiols, and ammonia.[15] It is therefore not clear if the *m/z* 74 and 106 ion−molecule products are also complexes or covalently bounded ions. Nevertheless, the fact that the CA spectra of these ions are dominated by fragments at *m/z* 44 and 76, respectively, is indicative of the covalent bonding, as the ionization energies of CS and CS_2 are higher than the ionization energy of nitric oxide. Whatever the

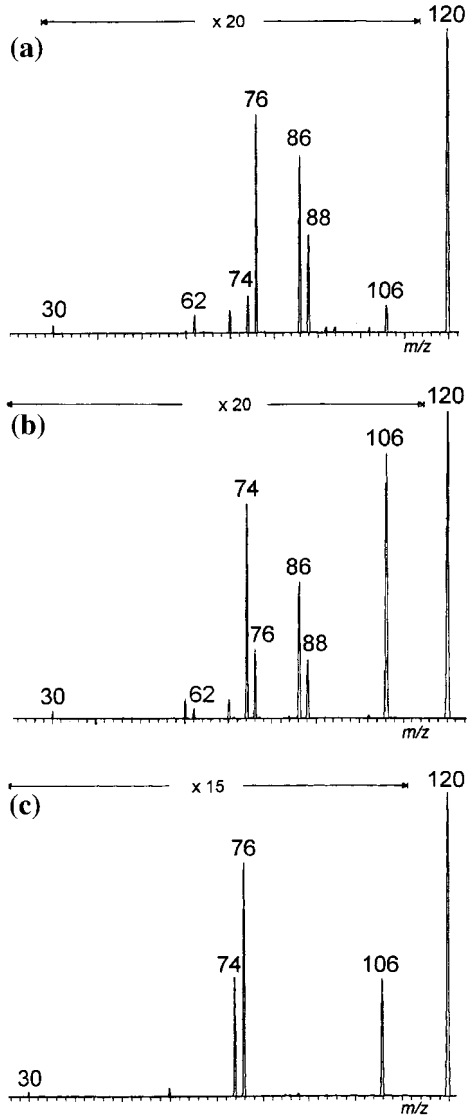

Figure 1. Ion−molecule reactions between the *m*/*z* 120 ions of **1** (a), **2** (b), **3** (c), and nitric oxide. Mass spectra (B scan) of the products generated in the quadrupole collision cell after reacceleration at 8 keV.

TABLE 3: Relative Abundances of the Principal Ions Observed in the CA Spectra (O_2 Collision Gas, 8 keV, Linked Scan Mode) of the Ion−Molecule *m*/*z* 106, 86, and 74 Products

	m/*z*						
precursor	76	70	58	56	44	32	30
m/*z* 106	100				7	3	10
m/*z* 86		13	100	41	20	10	29
m/*z* 74					100	6	30

actual structure of these ions, the fact that NO• displaces S_2, CS, and CS_2 may be indicative of the occurrence of a mixture of isomers such as $SCCSS^{\bullet+}$ (**5**) and $SCCS_2^{\bullet+}$ (**4**).

The reactivity of the *m*/*z* 120 ions generated by dissociative ionization of the dione **3** toward NO• is quite different; the peak at *m*/*z* 86 has now disappeared almost quantitatively, and the ratio *m*/*z* 106/*m*/*z* 74 is in fact very similar to the ratio observed in the case of **1** (Figure 1c). We propose, therefore, that the *m*/*z* 106 and 74 ion−molecule products can be attributed to *C*-sulfide ethenedithione ions, $S{=}C{=}CS_2^{\bullet+}$ (**4**), while the *m*/*z* 86 ion−molecule product results from the interaction of *S*-sulfide ethenedithione ions, $S{=}C{=}C{=}S{-}S^{\bullet+}$ (**5**), with nitric oxide (Scheme 2).

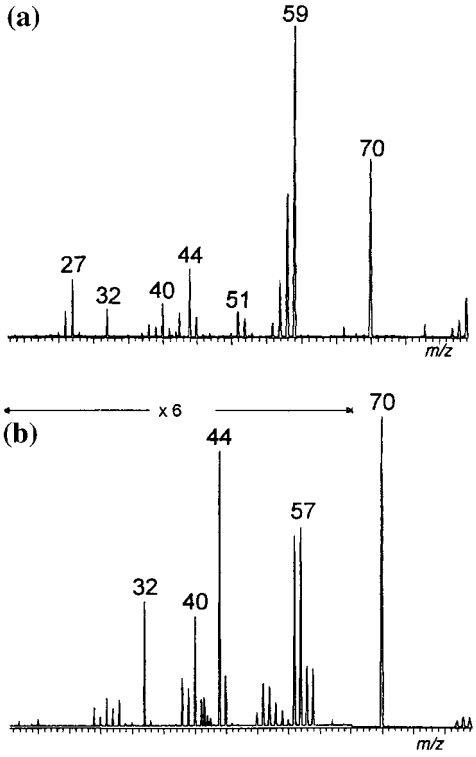

Figure 2. CA spectra (linked scan E/B/E mode) of the *m*/*z* 85 ions produced in the ion−molecule reaction of $C_2S_3^{\bullet+}$ ions (from **3**) with acetonitrile (a) and with methyl isocyanide (b).

SCHEME 2

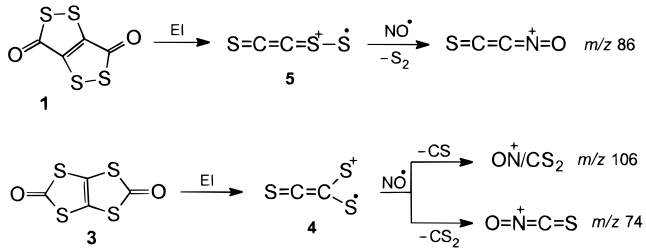

The behavior of the *m*/*z* 120 ions derived from **2** appears to be intermediate between **1** and **3**, again in agreement with the production of a mixture of isomers in different proportions (Figure 1b). It is worthy to note that $CS_3^{\bullet+}$ ions or the cumulogue $C_3S_3^{\bullet+}$ ions react also with nitric oxide in the quadrupole collision cell, but the major product ion is in these cases ONS^+ (*m*/*z* 62).[1,3] It is proposed that the reactive species are in these cases $SCSS^{\bullet+}$ and $SCCCSS^{\bullet+}$ ions, respectively, with the losses of the stable SCS or reasonably stable SCCCS cumulenes. The same reaction for the $SCCSS^{\bullet+}$ should be the loss of ethenedithione, SCCS, a less stable cumulene having an even number of carbon atoms.

Acetonitrile also reacts with the $C_2S_3^{\bullet+}$ ions from **1**−**3** producing with an excellent yield $[CH_3CN + CS]^{\bullet+}$ ions (*m*/*z* 85) by displacement of CS_2 with acetonitrile. The CA spectrum of these ion−molecule products shown in Figure 2a features very intense peaks for the losses of 15 and 26 Da ascribed to the losses of a methyl radical and ethyne, respectively, owing to the use of acetonitrile-d_3 in the ion−molecule reaction (*m*/*z* 88 fragmenting into *m*/*z* 70 and *m*/*z* 60). In fact, this spectrum is not very different from the spectrum of the $CH_3CNS^{\bullet+}$ ions[3] with the displacement of the main peaks by 12 Da. It is therefore proposed that they have the CH_3CNCS connectivity and result from the displacement of carbon disulfide by acetonitrile in the $S{=}C{=}CS_2^{\bullet+}$ species (**4**).

SCHEME 3

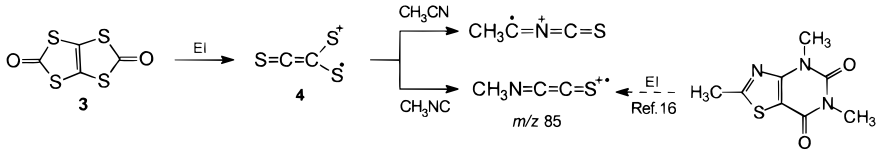

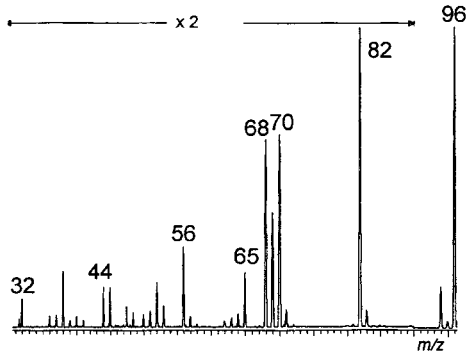

Figure 3. CA (linked scan E/B/E mode) spectrum of the *m/z* 97 ions produced in the ion−molecule reaction of $C_2S_3^{\bullet+}$ ions (from **3**) with methyl isocyanide.

Another reaction of importance when $C_2S_3^{\bullet+}$ ions (from **3**) react with acetonitrile is the displacement of CS producing *m/z* 117 ions; the structure of these ions associates therefore the elements of CH_3CN and CS_2.

Further confirmation of the CH_3CNCS connectivity for the *m/z* 85 ions was found in the study of the reaction of the $C_2S_3^{\bullet+}$ ions of **3** with methyl isocyanide. The *m/z* 85 ions are also readily produced in the quadrupole, and the CA spectrum of these ions (Figure 2b) differs very significantly from the spectrum shown in Figure 2a. Indeed, the *m/z* 59 peak is no longer significant, and the most intense fragmentation is the loss of a methyl group. In fact, this spectrum is identical to the spectrum of $CH_3NCCS^{\bullet+}$ radical cations published previously and prepared by dissociative ionization of a thiazolopyrimidine dione (Scheme 3).[16]

Beside the *m/z* 85 ions, we also observed the prominent production of *m/z* 97 and 117 ions assigned to the CH_3NC + CCS (displacement of disulfur) and CH_3NC + CS_2 (displacement of CS) compositions, respectively. The variation of the abundance ratios of the *m/z* 85, 97, and 117 ions on going from **1** to **3** suggests again that the $SCCCS^{\bullet+}$ and $SCCS_2^{\bullet+}$ radical cations are present in different proportions and that the $SCCS_2^{\bullet+}$ ions (**4**) react predominantly with methyl isocyanide by displacement of CS_2 (*m/z* 85) or CS (*m/z* 117) while the $SCCSS^{\bullet+}$ ions (**5**) react by displacement of S_2 (*m/z* 97).

The CA spectrum of the *m/z* 97 ions (Figure 3) features a base peak for the loss of $H^{\bullet}$ (*m/z* 96), an intense loss of $CH_3^{\bullet}$ (*m/z* 82), a series of peaks corresponding to (poly)carbon sulfides (*m/z* 68, 56, 44) and a characteristic loss of sulfur (*m/z* 65). All these fragmentations are in good accordance with the proposed cumulenic structure, $CH_3N{=}C{=}C{=}C{=}S^{\bullet+}$. The loss of CHN (*m/z* 70) must be the result of a rearrangement process. Iminopropadiene thione ions have not yet been reported in the literature, while iminopropadienone ions are well-established species.[17,18]

Summarizing the experimental results, dissociative ionization of the heterocyclic dithiolodithioles **1**−**3** generates mixtures of isomeric $C_2S_3^{\bullet+}$ radical cations ascribed as *S*- and *C*-sulfide ions derived from ethenedithione (**5** and **4**, respectively). These species cannot be differentiated with their collisional activation spectra in the high or the low kinetic energy regime nor with the neutralization−reionization methodology. In sharp contrast, ion−molecule reactions, in particular with nitric oxide, clearly indicate the production of $SCCSS^{\bullet+}$ and $SCCS_2^{\bullet+}$ radical cations. Upon reaction with acetonitrile or methyl isocyanide, the $SCCS_2^{\bullet+}$ ions are shown to produce isomeric $CH_3CNCS^{\bullet+}$ and $CH_3NCCS^{\bullet+}$ radical cations. Cumulenic $CH_3NCCCS^{\bullet+}$ radical cations have also been unambiguously characterized by collisional activation.

Molecular Orbital Calculations

1. Computational Methods. Standard ab initio calculations were carried out with the GAUSSIAN 94 series of programs.[19] The structures and energies of $C_2S_3^{\bullet+}$ radical cations and related fragments and ion−molecule reaction products were examined at the G2(MP2,SVP) level of theory.[20] This corresponds effectively to QCISD(T)/6-311+G(3df,2p)//MP2/6-31G* energies together with zero-point vibrational and isogyric corrections. Spin-restricted calculations were used for closed-shell systems, and spin-unrestricted ones for open-shell systems.

2. $C_2S_3^{\bullet+}$ Isomeric Structures. Ethenedithione, S=C=C=S, has three possible sites of sulfuration, namely, *C*-sulfurated ($SCCS_2^{\bullet+}$, **4**), *S*-sulfurated ($SCCSS^{\bullet+}$, **5**), and *CC*-sulfurated ions ($SC(S)CS^{\bullet+}$, **6**) (Figure 4). The *CC*-sulfurated ion (**6**) corresponds to a three-membered ring structure. The most stable $C_2S_3^{\bullet+}$ ion is the *C*-sulfurated form (**4**). The cyclic structure (**6**) lies close in energy (8 kJ mol^{-1} above **4**), while the *S*-sulfurated form (**5**) is significantly higher in energy (91 kJ mol^{-1} above **4**). Rearrangement of the *S*-sulfurated ion (**5**) to the more stable *C*-sulfurated form (**4**), via a 1,2-S shift transition structure **7** (Figure 4), has a significant activation barrier of 72 kJ mol^{-1}. On the other hand, rearrangement of the cyclic structure **6** to **4**, via transition structure **8**, has a small barrier of 33 kJ mol^{-1}. Thus, **4** and **5** are predicted to be observable $C_2S_3^{\bullet+}$ ions in the gas phase, while the cyclic structure (**6**) is unlikely to be experimentally accessible. The greater stability of **4** and **6** may be explained by the fact that the central carbon atoms of S=C=C=S bear strong negative charges and are the most probable sites of sulfuration.[21] The calculated atomic charges, based on natural bond orbital (NBO) analysis,[22] of the carbon and sulfur atoms in S=C=C=S are −0.25 and 0.25, respectively.

There are some interesting structural features of the $C_2S_3^{\bullet+}$ ions that warrant discussion. The *C*-sulfurated ion (**4**) is characterized by a rather short CS bond (1.493 Å, Figure 4). For comparison, the CS bond length in carbon sulfide is 1.546 Å (MP2/6-31G*). In addition, **4** is calculated to have large SCC bond angles (139°). In fact, the S···S distance (2.221 Å) is significantly less than the sum of the van der Waals radii. The *S*-sulfurated ion (**5**) has a long S−S bond length (1.991 Å), similar to that in carbon disulfide *S*-sulfide ion ($SCSS^{\bullet+}$) (2.034 Å),[3] which suggests that S−S bond cleavage in **5** is rather easy. For the cyclic structure (**6**), the C−C and C−S bond distances in the three-membered ring (Figure 4) are close to that of a typical single bond.

3. Fragmentation Energies of 4 and 5. We have calculated the unimolecular fragmentation energies of the $SCCS_2^{\bullet+}$ (**4**) and $SCCSS^{\bullet+}$ (**5**) radical cations using the G2(MP2,SVP) theory

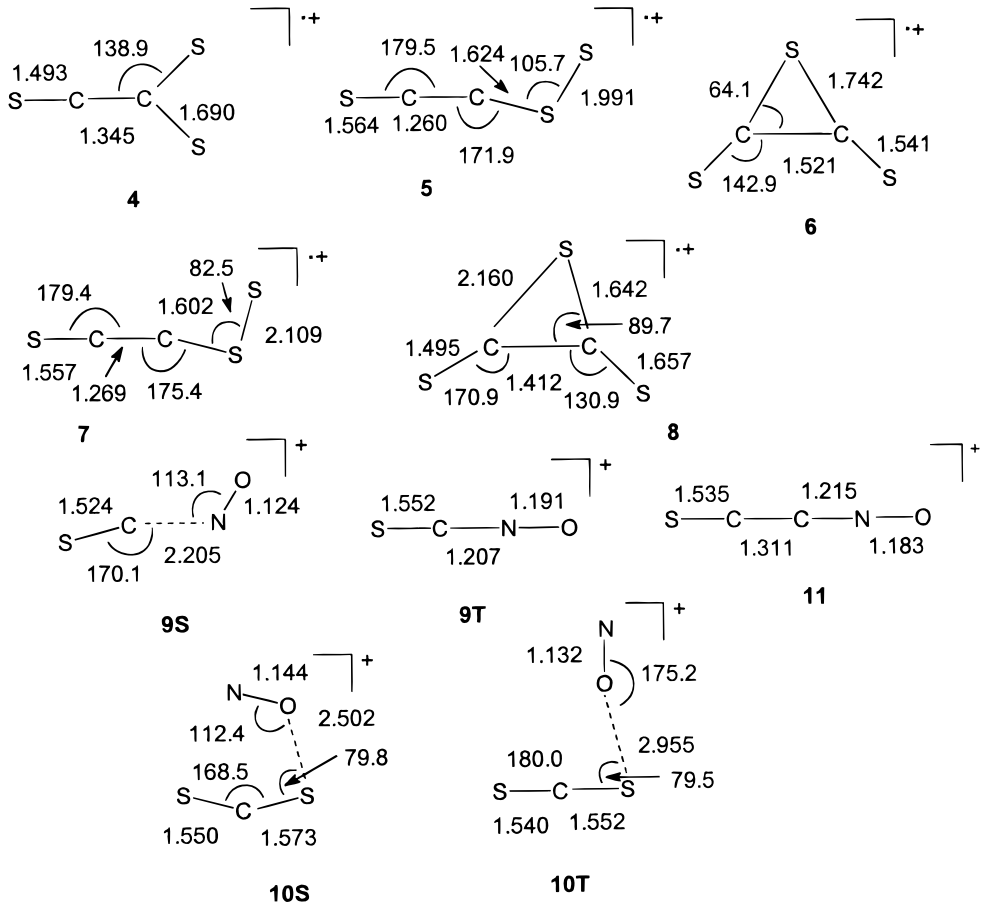

Figure 4. Optimized (MP2/6-31G*) equilibrium and transition structures of $C_2S_3^{\bullet+}$ ions and related fragments (bond lengths in Å and bond angles in degrees).

TABLE 4: Calculated Fragmentation Energies (kJ mol^{-1})[a] of $SCCS_2^{\bullet+}$ (4) and $SCCSS^{\bullet+}$ (5)

species	relative energy	species	relative energy
$SCCS_2^{\bullet+}$ (**4**)	0.0	$SCCSS^{\bullet+}$ (**5**)	0.0
$SC(S)CS^{\bullet+}$ (**6**)	9.4	$CS + CSS^{\bullet+}$ (*m*/*z* 76)	35.0
$SCCSS^{\bullet+}$ (**5**)	91.3	$S + SCCS^{\bullet+}$ (*m*/*z* 88)	264.4
$CS + CS_2^{\bullet+}$ (*m*/*z* 76)	131.2	$CCS + S_2^{\bullet+}$ (*m*/*z* 64)	415.0
$CS_2 + CS^{\bullet+}$ (*m*/*z* 44)	258.5	$CSS + CS^{\bullet+}$ (*m*/*z* 44)	453.1
$S + SCCS^{\bullet+}$ (*m*/*z* 88)	355.7	$S_2 + CCS^{\bullet+}$ (*m*/*z* 56)	461.0
$SCCS + S^{\bullet+}$ (*m*/*z* 32)	631.1	$SCCS + S^{\bullet+}$ (*m*/*z* 32)	539.9
$S + CCS_2^{\bullet+}$ (*m*/*z* 88)	737.5	$S + CCSS^{\bullet+}$ (*m*/*z* 88)	696.2
$CCS_2 + S^{\bullet+}$ (*m*/*z* 32)	744.0	$CCSS + S^{\bullet+}$ (*m*/*z* 32)	765.9

[a] G2(MP2,SVP) level. G2(MP2,SVP) E_0 energies include −1269.90970 (**4**) and −1269.87494 (**5**) hartrees.

(Table 4). Dissociation to $CS + CS_2^{\bullet+}$ (*m*/*z* 76) represents the lowest-energy fragmentation process of the *C*-sulfurated ion (**4**). Loss of CS_2 is the next most favorable dissociation reaction. The simple bond C−S cleavage processes are less favorable. Although the *S*-sulfurated form (**5**) is characterized by a long S−S bond, the simple S−S bond cleavage, giving $SCCS^{\bullet+}$ (*m*/*z* 88), is the second most favorable fragmentation process. The lowest-energy dissociation pathway corresponds to the C−C cleavage, giving $CS + CS_2^{\bullet+}$ (*m*/*z* 76). Other fragmentation processes are significantly higher in energy (Table 4). It is worth noting that the loss of CS for both **4** and **5** requires significantly less energy than other fragmentation processes. Thus, **4** and **5** are expected to have a very intense peak at *m*/*z* 76 in the respective CA spectrum. This result is in good accord with the observed spectra (Table 1). Since isomerization between **4** and **5** has a moderate energy barrier, it is likely that their CA spectra are complicated by the rearrangement process. As a consequence, it is not straightforward to deduce the structures of the two isomeric $C_2S_3^{\bullet+}$ ions simply from their CA mass spectra.

TABLE 5: Calculated Reaction Enthalpies[a] for Reaction of $SCCS_2^{\bullet+}$ (4) and $SCCSS^{\bullet+}$ (5) with NO$^{\bullet}$

$SCCS_2^{\bullet+}$ (**4**) + NO$^{\bullet}$		$SCCSS^{\bullet+}$ (**5**) + NO$^{\bullet}$	
product[b]	ΔE	product[b]	ΔE
$CS + S_2CNO^+$ (T)	−58.4	$SCCNO^+ + S_2$ (T)	−98.4
$SCNO^+$ (T) + CS_2	−10.0	SCCS (T) + SNO^+	−37.6
SCCS (T) + SNO^+	53.7	$CS + SSCNO^+$	56.8
$SNO^+ + CCS_2$	178.8	$SCNO^+$ (T) + CSS	184.5
S (T) + S_2CCNO^+	203.3	CCSS + SNO^+	200.8
$SCCSNO^+ + S$ (T)	*c*	CCS + $SSNO^+$	282.0
		$SCCSNO^+ + S$ (T)	*c*
		$SSCCNO^+ + S$ (T)	*c*

[a] G2(MP2,SVP) values (in kJ mol^{-1}). [b] T denotes triplet state. [c] $SCCSNO^+$ and $SSCCNO^+$ do not exist as a stable species.

4. Ion−Molecule Reactions with NO$^{\bullet}$. We have considered all possible reactions between the $C_2S_3^{\bullet+}$ ions and nitric oxide (NO$^{\bullet}$). The calculated reaction enthalpies for the ion−molecule reactions are summarized in Table 5. For the *S*-sulfurated ion (**5**), cleavage of the C−S bond, leading to the formation of $SCCNO^+$ and S_2, is calculated to be the most favorable reaction ($\Delta E = -98$ kJ mol^{-1}). Cleavage of the S−S bond in **5** leading to the formation of SNO^+ is also calculated to be an exothermic process. This result is in excellent agreement with the experimental observation. The ion−molecule reaction of the *C*-sulfurated ion (**4**) with NO$^{\bullet}$ is predicted to have different products than the corresponding reaction of the *S*-sulfurated form. C−C cleavage in **4** leading to the formation of triplet S_2CNO^+ or $SCNO^+$ is the most favorable reaction pathway

TABLE 6: Calculated Fragmentation Energies (kJ mol^{-1})[a] of $SCNO^+$ (9T), S_2CNO^+ (10T), and $SCCNO^+$(11)

species[b]	relative energy	species[b]	relative energy
$SCNO^+$ (T) (**9T**) (*m*/*z* 74)	0.0	$SCCNO^+$ (**11**) (*m*/*z* 86)	0.0
$NO^\bullet + CS^{\bullet+}$ (*m*/*z* 44)	268.5	$CCS + NO^+$ (*m*/*z* 30)	460.4
CS (T) $+ NO^+$ (*m*/*z* 30)	410.7	$NO^\bullet + SCC^{\bullet+}$ (*m*/*z* 56)	505.5
		$O + SCCN^+$ (*m*/*z* 70)	502.3
S_2CNO^+ (T) (**10T**) (*m*/*z* 106)	0.0	$CNO^\bullet + CS^{\bullet+}$ (*m*/*z* 44)	604.6
$NO^\bullet + C_2S^{\bullet+}$ (*m*/*z* 76)	189.6	$CS + CNO^+$ (*m*/*z* 42)	679.8
CS_2 (T) $+ NO^+$ (*m*/*z* 30)	389.5	$S + CCNO^+$ (*m*/*z* 54)	766.3
		$CCNO^\bullet + S^{\bullet+}$ (*m*/*z* 32)	936.2
		$SCCN^\bullet + O^{\bullet+}$ (*m*/*z* 16)	1182.9

[a] G2(MP2,SVP) level. G2(MP2,SVP) E_0 energies include −565.12552 (**9T**), −962.95208 (**10T**), and −603.19524 (**11**) hartrees. [b] T denotes triplet state.

(Table 5). The formation of SNO^+ in this case is a slightly endothermic process, in contrast to the case for the *S*-sulfurated ion. Again, the theoretical finding is in good accord with the experimental result. In summary, the calculated energetics for reaction of **4** and **5** confirm the experimental finding that the two forms of $C_2S_3^{\bullet+}$ ions could be differentiated by ion−molecule reaction with nitric oxide.

There are interesting fragmentation patterns for the above ion−molecule reaction products, namely, $SCNO^+$ (**9**), S_2CNO^+ (**10**), and $SCCNO^+$ (**11**), that warrant discussion. Singlet (**9S**) and triplet (**9T**) $SCNO^+$ ions are predicted to have quite different structures (Figure 4).[13] The singlet $SCNO^+$ ion (**9S**) is characterized by a very long C−N bond length (2.205 Å) and is best considered as an ion−molecule complex between CS and NO^+. The triplet structure (**9T**), on the other hand, is a covalently bonded species (S═C═N^+═O) with a C═N double length of 1.207 Å. **9S** is more stable than **9T** by 38 kJ mol^{-1}. We have shown recently that both the singlet and triplet could be observed in the CA spectra and the use of oxygen collision gas significantly increase the contribution of the triplet state.[13] Dissociation of **9T** to $NO^\bullet + CS^{\bullet+}$ (*m*/*z* 44) is calculated to be a more energetically favorable process than fragmentation to $CS + NO^+$ (*m*/*z* 30) (Table 6), in excellent accord with the observed CA spectrum (Table 3).

For $[S_2CNO]^+$ (**10**), both the singlet (**10S**) and triplet (**10T**) states are predicted to be weakly bonded $[C_2S{-}NO]^+$ complexes (Figure 4), with the singlet state being slightly preferred by 25 kJ mol^{-1}. The "normal" covalently bonded species are significantly higher in energy. In agreement with experiment (Table 3), loss of $NO^\bullet$, giving $CS_2^{\bullet+}$ (*m*/*z* 76), in the triplet S_2CNO^+ (**10T**) is energetically more favorable than loss of CS_2 to give NO^+ (*m*/*z* 30).

$SCCNO^+$ (**11**) is predicted to have a singlet ground state and has a normal covalent structure (S═C═C═N^+═O) (Figure 4). The calculated fragmentation energies of **11** (Table 6) agree well with the CA spectrum (Table 3). The *m*/*z* 58 ions ($NCS^{\bullet+}$) in the CA spectrum may arise from the fragmentation of the isomeric $[NO{-}CCS]^+$ complex, which could be formed by addition of $NO^\bullet$ to the C═C double bond of the $CCS^{\bullet+}$ ion. Hence, the calculated fragmentation patterns of **9T**, **10T**, and **11** strongly support the assignment of their structures in the CA spectra.

Conclusions

Collisional activation (CA), neutralization−reionization (NR), and ion−molecule reaction experiments making use of a hybrid tandem mass spectrometer have been used to investigate the structures of $C_2S_3^{\bullet+}$ isomers. The CA and NR spectra cannot be used to differentiate the structures of the isomeric $C_2S_3^{\bullet+}$ ions. On the other hand, ion−molecule reactions clearly indicate the production of $SCCS_2^{\bullet+}$ (**4**) and $SCCSS^{\bullet+}$ (**5**) radical cations. Ab initio calculations using the G2(MP2,SVP) theory support the existence of the two isomeric ions. The *C*-sulfide ethenedithione ion (**4**) is more stable than the *S*-sulfide form (**5**) by 91 kJ mol^{-1}. The calculated reaction enthalpies for **4** and **5** reacting with $NO^\bullet$ are in excellent accord with experimental findings. The calculated fragmentation energies of ion−molecule products confirmed the structural assignment of their CA spectra.

Acknowledgment. The Mons laboratory thanks the "Fonds National de la Recherche Scientifique" for its contribution in the acquisition of the large scale tandem mass spectrometer and for financial support (fellowship for P.G.). Prof. E. Fanghänel (Martin-Luther-Universität, Halle-Wittenberg) is greatly acknowledged for providing us a sample of the dithiolodithiole **2**. M.W.W. thanks the National University of Singapore for financial support (Grant 970620).

References and Notes

(1) Th. Pedersen, C.; Flammang, R.; Gerbaux, P.; Fanghänel, E. *J. Chem. Soc., Perkin 2* **1998**, 350.
(2) Sülzle, D.; Schwarz, H. *Chem. Ber*. **1989**, *122*, 1803.
(3) Gerbaux, P.; Van Haverbeke, Y.; Flammang, R.; Wong, M. W.; Wentrup, C. *J. Phys. Chem. A* **1997**, *101*, 6970.
(4) Flammang, R.; Van Haverbeke, Y.; Braybrook, C.; Brown, J. *Rapid Commun. Mass Spectrom*. **1995**, *9*, 795.
(5) Gerbaux, P.; Van Haverbeke, Y.; Flammang, R. *J. Mass Spectrom*. **1997**, *32*, 1170.
(6) Bateman, R. H.; Brown, J.; Lefevere, M.; Flammang, R.;. Van Haverbeke, Y. *Int. J. Mass Spectrom. Ion Processes* **1992**, *115*, 205.
(7) Richter, A. M.; Fanghänel, E. *Tetrahedron Lett*. **1983**, *24*, 3577.
(8) Goldberg, N.; Schwarz, H. *Acc. Chem. Res*. **1994**, *27*, 347.
(9) Schalley, C. A.; Hornung, G.; Schröder, D.; Schwarz, H. *Chem. Soc. Rev*. **1998**, *27*, 91.
(10) Stirk, K. M.; Orlowski, J. C.; Leeck, D. T.; Kenttämaa, H. I. *J. Am. Chem. Soc*. **1992**, *114*, 8604.
(11) Gerbaux, P.; Flammang, R.; Nguyen, M. T.; Salpin, J.-Y.; Bouchoux, G. *J. Phys. Chem. A* **1998**, *102*, 861.
(12) Lias, S. G.; Bartmess, J. E.; Liebman, L. F.; Holmes, J. L.; Levin, R. D.; Mallard, W. G. *J. Phys. Chem. Ref. Data* **1988**, *17*, (Suppl. 1).
(13) Flammang, R.; Gerbaux, P.; Wong, M. W. *Chem. Phys. Lett*. **1999**, *300*, 183.
(14) Wong, M. W.; Wentrup, C.; Mørkved, E. H.; Flammang, R. *J. Phys. Chem*. **1996**, *100*, 10536.
(15) Nguyen, M. T.; Lahem, D.; Flammang, R. *Chem. Phys. Lett*. **1998**, *283*, 357.
(16) Flammang, R.; Landu, D.; Laurent, S.; Barbieux-Flammang, M.; Kappe, C. O.; Wong, M. W.; Wentrup, C. *J. Am. Chem. Soc*. **1994**, *116*, 2005.
(17) Flammang, R.; Laurent, S.; Flammang-Barbieux, M.; Wentrup, C. *Rapid Commun. Mass Spectrom*. **1992**, *6*, 667.
(18) Mosandl, T.; Stadtmüller, S.; Wong, M. W.; Wentrup, C. *J. Phys. Chem*. **1994**, *98*, 1080.
(19) Frisch, M. J.; Trucks, G. W.; Schlegel, H. B.; Gill, P. M. W.; Johnson, B. G.; Robb, M. A.; Cheeseman, J. R.; Keith, T.; Petersson, G. A.; Montgomery, J. A.; Raghavachari, K.; Al-Laham, M. A.; Zakrzewski, V. G.; Ortiz, J. V.; Foresman, J. B.; Cioslowski, J.; Stefanov, B. B.; Nanayakkara, A.; Challacombe, M.; Peng, C. Y.; Ayala, P. Y.; Chen, W.; Wong, M. W.; Andres, J. L.; Replogle, R. E.; Gomperts, R.; Martin, R.; Fox, D. J.; Binkley, J. S.; DeFrees, D. J.; Baker, J.; Stewart, J.J. P.; Head-Gordon, M.; Gonzalez C.; Pople, J. A. *GAUSSIAN 94*; Gaussian Inc.: Pittsburgh, PA, 1995.
(20) Curtiss, L. A.; Redfern, P. C.; Smith, B. J.; Radom, J. *Chem. Phys*. **1996**, *104*, 5148.
(21) Ma, N. L.; Wong, M. W. *Angew. Chem., Int. Ed. Engl*. **1998**, *37*, 3402. Wong, M. W.; Flammang, R.; Wentrup, C. *J. Phys. Chem*. **1995**, *99*, 16849.
(22) Reed, A. E.; Curtiss, L. A.; Weinhold, F. *Chem. Rev*. **1988**, *88*, 899.